Reviews of Electromagnetics, Vol. IV, 2025
EuCAP 2025 Special Issue
DOI: 10.53792/RoE/2025/25011

Reviews of Electromagnetics
EuCAP 2025 Special Issue

Slant-Polarized Coaxial Slot Antenna Using Gap Waveguide MLW Technology for Automotive Radars

Reza Gheybi Zarnagh[1]*, Abolfazl Haddadi[2], Andrés Alayón Glazunov[3]

Abstract
This paper presents the design of a coaxial slot antenna utilizing gap waveguide (GW) multilayer waveguide (MLW) technology for automotive radar applications. The antenna employs a low-loss, air-filled coaxial transmission line, formed by stacking three distinct metal sheets. Its primary antenna element is a side-fed column featuring eight in-line slant slots, each pair excited via a coupling slot and intermediate cavity. To minimize leakage caused by small air gaps between the metal sheets, an electromagnetic bandgap (EBG) structure is incorporated along the transmission lines. The antenna supports dedicated transmit and receive channels for a multiple-input multiple-output (MIMO) automotive radar system. A five-layer structure progressively rotates the electric field orientation by 45° through intermediate cavities, enabling the slant polarization. The design achieves an impedance bandwidth of $|S_{11}| < -10$ dB across the 76–81 GHz band allocated for automotive radar. With eight radiating slots, the antenna produces a peak gain of 13.7 dBi at 77 GHz.

Key terms
Radar applications; Multilayer Waveguide (MLW); slot array antenna; slant polarization

[1] *Department of Electrical Engineering, University of Twente, Enschede, The Netherlands*
[2] *Gapwaves AB, Gothenburg, Sweden*
[3] *Department of Science and Technology, Linköping University, Norrköping Campus, Sweden*
***Corresponding author**: r.gheybizarnagh@utwente.nl*

Received: 22/05/2025, Accepted: 20/07/2025, Published: 28/11/2025

1. Introduction

Automotive radars have gained significant attention in advanced driver assistance systems (ADAS) due to their robustness in harsh weather conditions and their precision in detecting diverse targets [1], [2]. Operating at millimeter-wave (mmWave) frequencies significantly improves radar resolution and accuracy, enabling the detection of smaller objects. In particular, the E-band frequency range from 76 to 81 GHz is widely adopted in automotive radar applications due to its superior performance enabled by favorable propagation characteristics and large available bandwidth [3].

Fully polarimetric radar systems, which require dual orthogonal polarizations at both the transmitter (Tx) and receiver (Rx), are now being explored for automotive use [4]. Utilizing orthogonal polarizations can help reduce self-interference and mitigate coupling between subarray beams, which is especially critical for multi-function radar systems [5].

Most current automotive radars operate at 77 GHz frequencies to benefit from the wide bandwidth available at mmWave frequencies. However, larger arrays of antenna elements are necessary to meet increasing demands for higher antenna gain and additional Tx/Rx channels. A key challenge at these frequencies is minimizing dielectric loss. Gap waveguide (GW) antennas, with their fully metallic structure, provide a high-gain alternative to conventional hollow waveguides (see [6] and [7] for an overview). GWs effectively confine electromagnetic field wave propagation within a well-defined guiding structure, thus reducing dielectric and transmission losses [8], [9].

Another promising approach gaining traction for creating efficient millimeter-wave antennas is the multilayer waveguide (MLW) technique, recently introduced in [10]. This method offers an alternative to air-filled waveguides, allowing for reduced array element separation and eliminating the need for dielectric materials. The MLW supports the transverse electromagnetic (TEM) propagation mode through stacked, unconnected thin

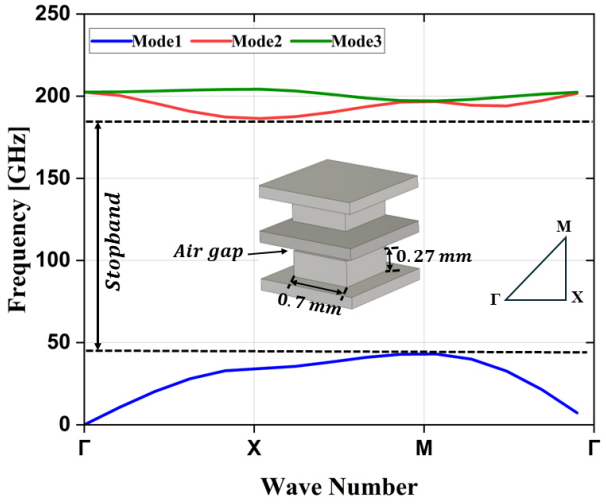

Figure 1: Dispersion diagram for the infinite periodic EBG unit cell.

Table 1: Dimensions of MLW coaxial slot antenna.

Parameter	W	L	Ch_w	S_w	Ch_{in}
Value (mm)	17	31	1.5	0.75	1.3
Parameter	S_{in}	g_t	$Slotc_t$	$Slotc_w$	$Slotc_l$
Value (mm)	0.75	0.44	1.45	0.47	2.17
Parameter	Cav_w	Cav_l	Cav_t	$Slotr_l$	$Slotr_w$
Value (mm)	2.1	3.5	0.95	2.27	0.45

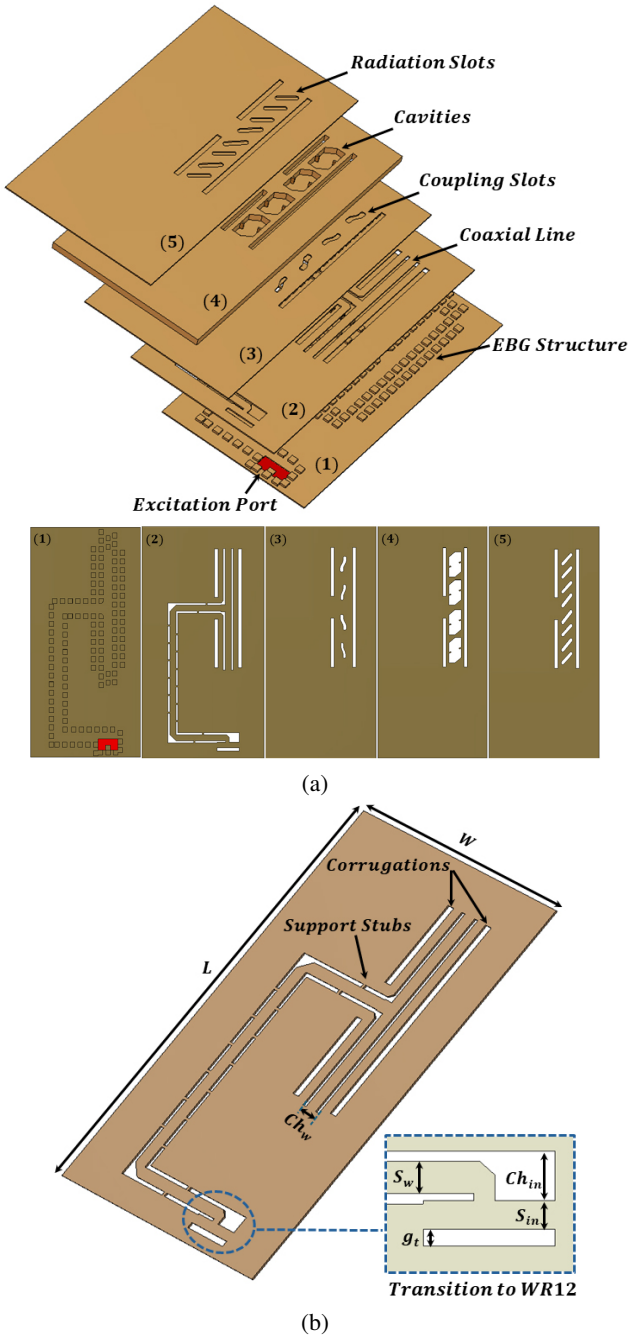

Figure 2: (a) MLW coaxial antenna configuration, (b) detailed structural view of the coaxial line.

metal sheets [11]. This allows for tighter element spacing in antenna arrays. A side-fed slot array based on MLW technology was presented in [12], where meandered slots were employed to facilitate excitation via the TEM mode, producing horizontal polarization.

The MLW technology allows for polarization control (including linear and slant), compact form factors, and tunable impedance through slot geometry and spacing. MLW-based antennas produce broadside radiation patterns and are well-suited for high-frequency applications such as mmWave radar and communication systems [11]. Moreover, MLW offers efficient radiation performance at millimeter-wave frequencies, making it ideal for high-frequency applications. It supports scalable array configurations for beamforming, exhibits low transmission losses—particularly in air-filled or metallic implementations—and provides strong mechanical stability, enabling precise fabrication and reliable integration into radar and communication systems [11], [12].

In this work, we introduce a novel multilayer waveguide (MLW) antenna design that achieves 45° slant polarization, marking a significant advancement in enabling polarization diversity for automotive radar systems. Unlike conventional MLW implementations that are limited to linear polarization, the proposed approach facilitates the generation of complementary ±45° slant polarizations, offering improved isolation and enhanced performance in hybrid and integrated radar platforms. A key design innovation is using a side-fed coaxial line to ensure uniform slot excitation, resulting in superior radiation pattern control and overall antenna performance.

The remainder of the paper is divided into the following sections. In Section 2, we present the design guidelines for the GW MLW coaxial antenna design. We first introduce the EBG unit cell design, which improves isolation between contiguous antenna layers. We then proceed with designing the MLW antenna and its components. Section 3 presents the simulation results describing the designed transition's reflection and transmission coefficients, the realized antenna gain of the multi-slot slant-polarized antenna, its reflection coefficient, radiation

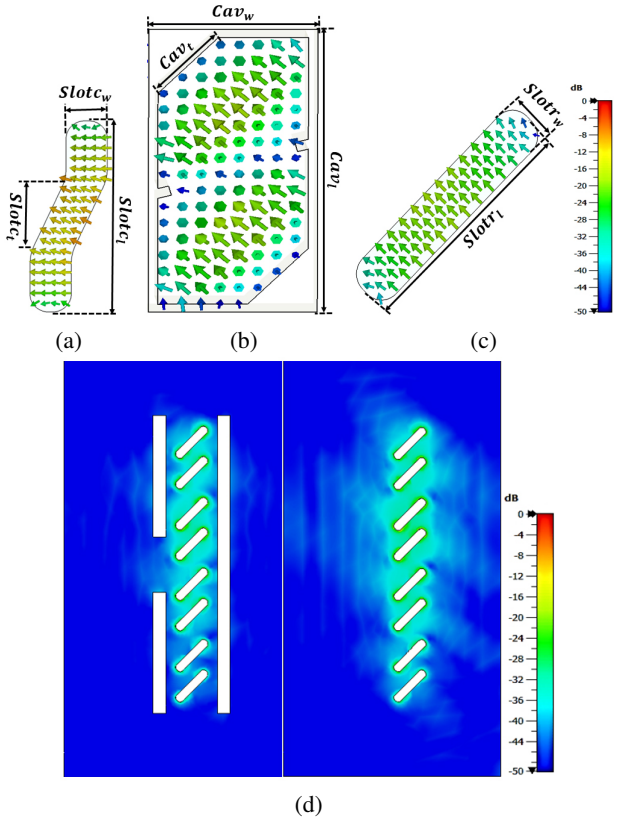

Figure 3: Electric field distribution, (a) on the coupling slot, (b) the cavity, (c) the radiating slot. (d) Surface current distribution with and without corrugations.

patterns, the front-to-back ratio, the side-lobe levels, and the cross-polarization ratio. We finalize with the conclusions.

2. MLW COAXIAL LINE ANTENNA DESIGN

An early version of this approach was introduced in [13] to reduce the spacing between array elements by eliminating the need for dielectric materials in coaxial lines supporting TEM mode propagation. This design incorporated small metal stubs along the coaxial line to provide mechanical support for the inner conductor. While functionally effective, the solution posed significant challenges in terms of manufacturing complexity and cost, rendering it impractical for large-scale manufacturing.

To overcome these limitations, a more scalable and easier to fabricate solution was proposed in [11], introducing the MLW technology. This technique employs a stack of multiple unconnected thin metal sheets. It utilizes chemical metal etching for precise and efficient manufacturing, enabling high-density array designs without compromising structural integrity or electrical performance. A lossy aluminium material (electrical conductivity $\approx 3.56 \times 10^7$ S/m) is considered in the design process of the natenna.

2.1. EBG Unit Cell

The concept of Electromagnetic Bandgap (EBG) structures has been extensively discussed in [14], where they are presented as an effective solution for creating bandgaps and suppressing unwanted electromagnetic wave propagation. In this work, the EBG unit cell was specifically engineered to operate within the E-band frequency range of 76–81 GHz. As illustrated in Fig. 1, the unit cell structure consists of a metallic pin with precisely optimised dimensions. A key feature of this design is the reduced pin height with respect to the traditional GW antennas, which demonstrates a notable advantage of the MLW approach—simplified fabrication and improved cost efficiency.

The dispersion diagram, also shown in Fig. 1, was generated using the CST Eigenmode solver. It reveals a wide bandgap extending from 43 GHz to 186 GHz within which no propagation modes exist. This wide stopband is achieved by incorporating a 10 μm air gap between metal layers, effectively suppressing undesired electromagnetic wave propagation. In this diagram, the vertical (y) axis represents frequency, while the horizontal (x) axis denotes the wave number. This broad stopband further emphasizes the design's effectiveness in suppressing unwanted electromagnetic wave propagation, highlighting its suitability for high-frequency applications.

2.2. MLW Coaxial Line Slot Array Antenna

This section outlines the design methodology for the proposed slant-polarized MLW coaxial slot array antenna. The overall configuration of the MLW coaxial line is depicted in Fig. 2(a), while Fig. 2(b) provides a detailed view of the structural components. The critical design parameters and physical dimensions of the antenna are summarized in Table 1, providing the foundation for the subsequent electromagnetic and fabrication performance analysis.

2.2.1. Main Structural Features

The antenna consists of five functional layers, each thoroughly designed to fulfill a specific role in achieving efficient slant-polarized radiation. These layers combine to guide, couple, and radiate energy with precise polarization control.

Bottom Layer (EBG Layer): This layer integrates periodic Electromagnetic Bandgap (EBG) unit cells formed on a thin metallic substrate. PIN-shaped EBG structures are strategically arranged along the coaxial transmission lines to suppress electric field leakage. These metallic EBG pins prevent the propagation of electromagnetic modes within the antenna's operational frequency band from 76–81 GHz, thereby effectively mitigating spurious radiation and enhancing signal integrity.

Second Layer (Coaxial Feed Layer): This layer forms the coaxial transmission line, with the inner conductor suspended between the adjacent bottom and top layers. It supports transverse electromagnetic (TEM) mode propagation and delivers power to the coupling slots in the upper layers.

Third Layer (Coupling Layer): This layer incorporates periodic EBG structures along with a thin metallic substrate etched with coupling slots. These slots enable efficient power transfer from the coaxial line to the radiation structure. The geometry and spacing of the slots are carefully optimized to ensure effective excitation by the desired TEM mode within the operating frequency band.

Fourth Layer (Cavity Layer): Strategically positioned cavities in this layer are designed to gradually rotate the electric fields by 45°, thereby initiating the polarization rotation needed

for slant-polarized radiation.

Top Layer (Radiation Layer): The top layer of the antenna incorporates slanted radiation slots, with corrugations along both sides of the antenna layers to effectively suppress surface wave leakage and minimize coupling between adjacent subarrays. These corrugations also enhance the azimuthal radiation pattern by reducing pattern ripple and mitigating ground plane effects, thereby improving the antenna gain. Significantly, due to the side-fed configuration of the coaxial line, the corrugations are strategically divided into two segments to avoid interference with the electromagnetic fields propagating within the coaxial feed structure. A comparison of surface current distributions, shown in Fig. 3(d), clearly demonstrates the significant impact on surface current behavior.

2.2.2. Additional Structural Features

Next, we describe the feeding structure and other specific design strategies implemented to achieve the desired radiated performance of the antenna.

A side-fed coaxial line is used to uniformly excite the radiating slots, enabling the integration of a larger number of elements and enhancing the overall radiation pattern performance. Unlike end-fed array configurations, which are prone to beam squint due to the frequency-dependent phase shifts across the aperture, the side-feeding effectively mitigates this issue [12].

The beam squint arises when the phase of the signal varies significantly with frequency, causing the main lobe to shift. The phase at a point on the antenna aperture for a given frequency f is expressed as [15]

$$\phi(f) = \frac{2\pi f l}{c}, \tag{1}$$

where l is the effective path length from the feed point to the radiating element, and c is the speed of light in free space. As frequency increases, the phase difference between adjacent elements becomes more pronounced, potentially distorting the main beam direction, as shown in [16].

The side-fed configuration reduces the effective electrical path length l (through which the wave must propagate to reach each slot), hence minimizing the phase variation across the aperture. This reduction significantly mitigates beam squint and contributes to more stable beam steering across the operational bandwidth.

Support stubs are introduced between the inner conductor and the surrounding structure of the coaxial feed to provide mechanical stability. Their positions are carefully optimized to minimize input reflection and maintain impedance matching at the feed port.

Each pair of radiation slots is excited via a meandered slot, with a center-to-center spacing of one guided wavelength (λ_g), ensuring in-phase excitation. While this spacing supports coherent radiation, it may also give rise to grating lobes under certain conditions. At this design stage, the polarization remains linear and oriented horizontally. Notably, the first two slots within the subarray are rotated by 180° around the y-axis to improve impedance matching.

Additional hexagonal cavities are embedded between layers to mitigate grating lobes and enable the generation of slant polarization. These cavities serve several purposes:

1. optimizing impedance matching,
2. enabling uniform power distributing to two slant-oriented radiation slots, and
3. mitigating grating lobes by disrupting periodicity in the array structure.

A slot spacing of $\lambda_g/2$ is employed between the slant-oriented slots to improve polarization purity and enhance overall antenna performance.

This multi-layered architecture effectively combines EBG-based filtering, precise electric field rotation, and efficient radiation, offering a robust solution for high-frequency slant-polarized antenna applications.

2.3. Routing and Rectangular Waveguide (RWG) to MLW Transition Designs

A transition from the standard WR-12 rectangular waveguide to MLW coaxial line was designed, building upon the concept proposed initially in [12]. This design provides mechanical and electromagnetic flexibility at the interface between the Launcher-in-Package (LiP) waveguide port and the corresponding antenna element. An exploded view of the proposed transition is shown in Fig. 2(b), while the simulated reflection and transmission coefficients of the transition are shown in Fig. 4(a).

Following the selection of the transition structure and antenna element configuration, a routing path from the LiP port to its respective antenna elements is carefully designed. To suppress signal leakage and reduce coupling between adjacent routing paths, a row of pins is placed along each transmission line. In cases where longer transmission lines are unavoidable, mechanical support structures, referred to as support stubs, are periodically integrated along the coaxial line. These stubs prevent structural deformation while being strategically spaced to avoid introducing reflections within the operating frequency band. An illustration of the routing layout is shown in Fig. 2(b).

3. SIMULATION RESULTS

The slot configurations across different layers, along with the simulated electric field distributions, are illustrated in Fig. 3 (similar to [17]). The first slotted layer, incorporating meandered slots, generates horizontal electric field components, as shown in Fig. 3(a). These components are subsequently rotated by 45° within the cavity layer, as depicted in Fig. 3(b). Effective coupling of the rotated fields to the slant-oriented slots is demonstrated in Fig. 3(c). Due to the in-phase excitation and the $\lambda_g/2$ spacing between the radiating slots, the antenna achieves a uniform radiation pattern.

Fig. 4 shows the simulated S-parameters and gain performance of the proposed antenna system, including the transition to a standard WR-12 waveguide. Fig. 4(a) shows the simulated reflection coefficient (S_{11}) and transmission coefficient (S_{21}) of the input transition from WR-12 to MLW coaxial line. The reflection coefficient remains below –20 dB across most of the 76–81 GHz band, indicating excellent impedance matching. The transmission coefficient is close to 0 dB, suggesting

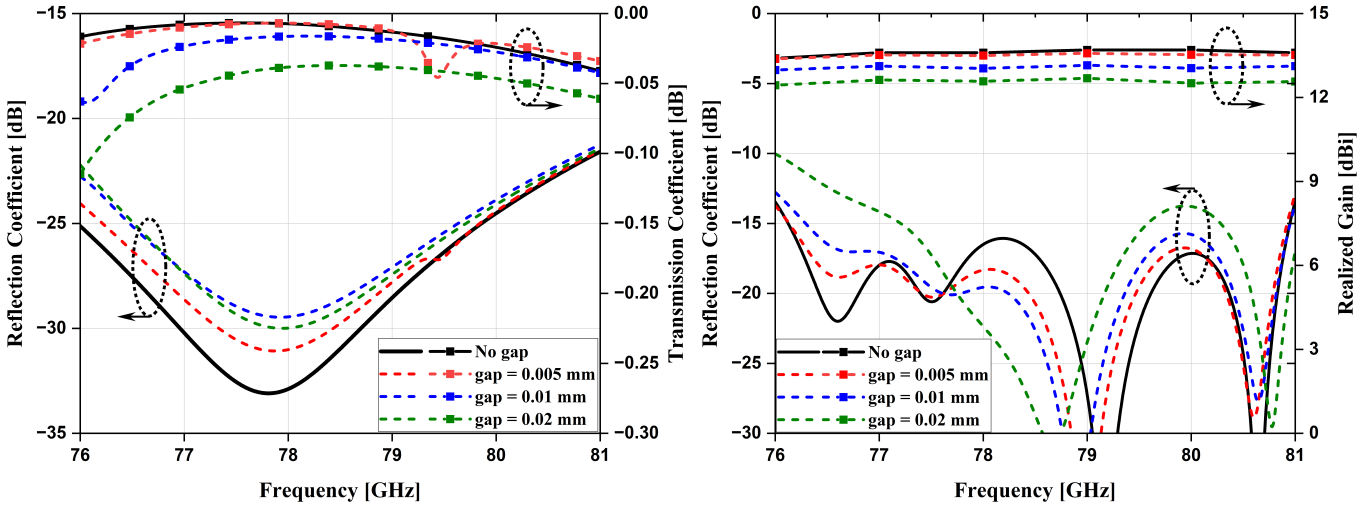

Figure 4: (a) Simulated reflection and transmission coefficients of the input transition to WR-12 plotted versus frequency. (b) Simulated reflection coefficient and gain of the proposed antenna versus frequency.

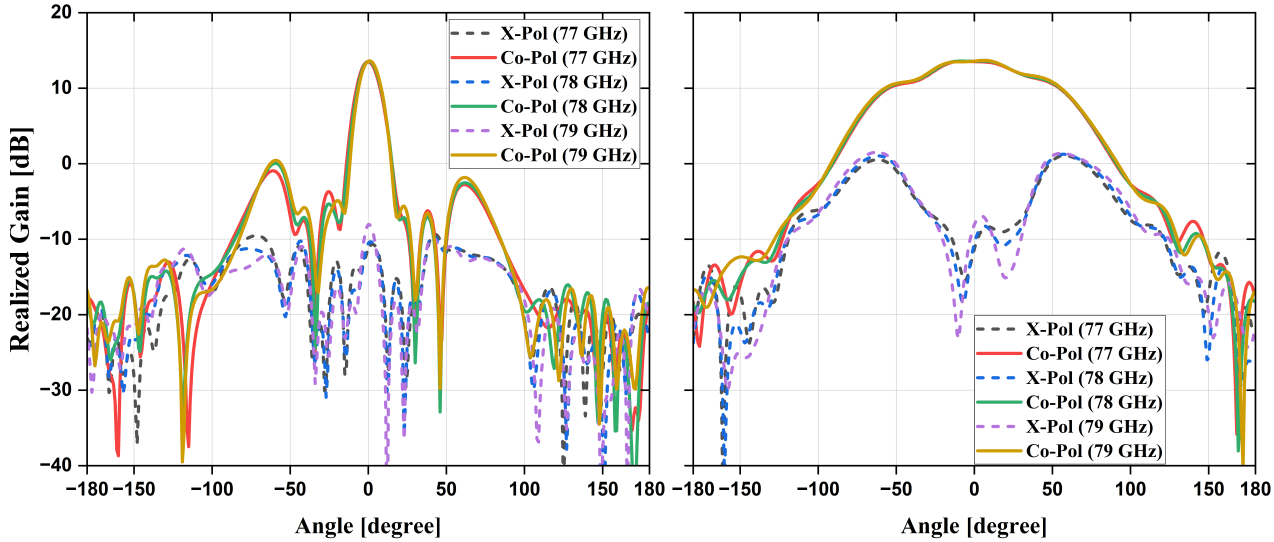

Figure 5: Co-polarized and X-polarized patterns of the simulated antenna versus angle at frequencies 77, 78, and 79 GHz, (a) E-plane and (b) H-plane.

Table 2: Comparison of the proposed antenna and previously reported works at E-band.

Ref	[5]	[11]	[12]	[16]	[18]	**This work**
Antenna type	GW	MLW	MLW	GW	MLW	**MLW**
Element number	1×2	2×6	1×6	8×18	3×8	**1×8**
Feeding topology	Series-Fed	End-Fed/Coaxial Line	Side-Fed/Coaxial Line	Series-Fed	Series (Center-fed)	**Side-Fed/Coaxial Line**
Bandwidth ($\lvert S_{11}\rvert < -10$ dB)	6.36%	6.36%	6.36%	3.9%	7.1%	**6.36%**
Peak Gain (dBi)	8.97	15	11.5	27.3	17	**13.7**
Side Lobe Level (dB)	-	<-14	-	<-15	<-15	<-15
HPBW (E-plane/H-plane)	-	-	20°/120°	-	16°/37°	14°/109°
Aperture efficiency	-	-	-	71.2%	76%	**95%**
Polarization	Slant	Horizontal	Horizontal	Circular	Horizontal	**Slant**
Thickness (mm)	4.8	0.95	0.95	6.53	1.9	**1.6**
Validation	Sim	Sim&Meas	Sim&Meas	Sim&Meas	Sim&Meas	**Sim**

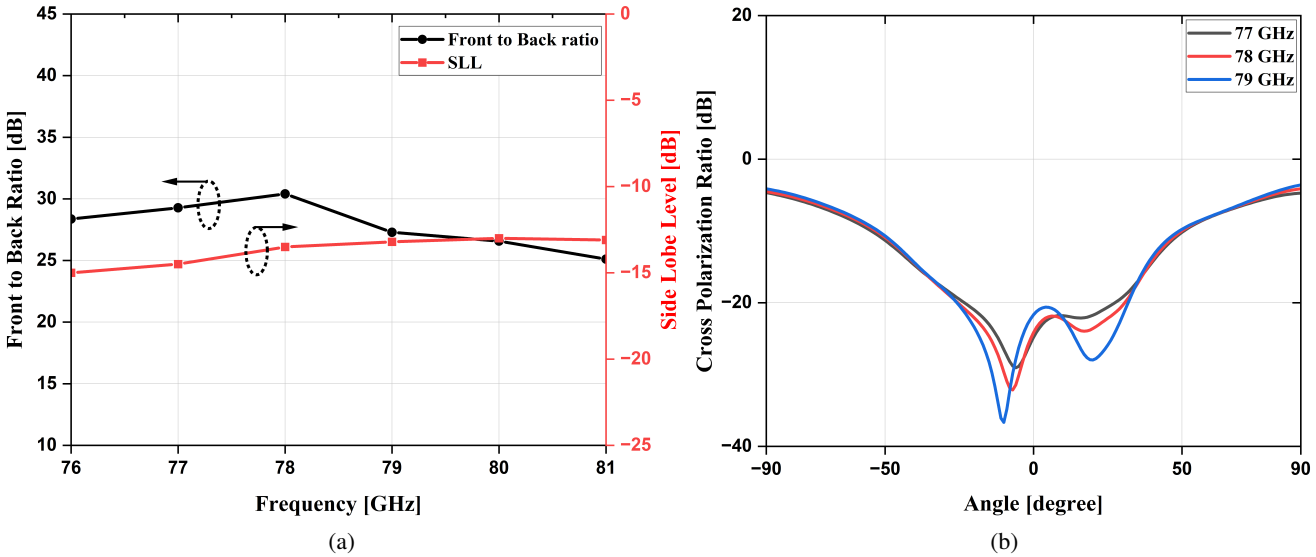

Figure 6: (a) Front to Back ratio and Side Lobe Level of the antenna versus frequency and (b) Cross Polarization ratio versus angle.

minimal insertion loss and efficient power transfer through the transition structure. Fig. 4(b) presents the reflection coefficient (S_{11}) of the antenna and realized broadside gain across the operating frequency range. The antenna exhibits excellent performance in the 76–81 GHz band, satisfying the $|S_{11}| < -10$ dB criterion typically required for automotive radar applications. The realized gain remains relatively flat across the band, averaging around 13.5 dBi, which confirms stable performance and effective radiation over the operating frequency range. A tolerance study has been conducted to evaluate the impact of varying air gap distances between the antenna layers.

The simulated E- and H-plane radiation patterns at 77, 78, and 79 GHz are shown in Fig. 5, while additional radiation characteristics are detailed in Fig. 6.

Fig. 5 shows the simulated radiation patterns of the proposed antenna in both the E-plane and H-plane at three operating frequencies: 77 GHz, 78 GHz, and 79 GHz. In the E-plane (Fig. 5(a)), the co-polarized gain is significantly higher than the cross-polarized gain across all angles, i.e., with a Cross-Polar Discrimination $XPD > 24.6$ dB, confirming strong polarization purity and consistent directional performance. The main lobe of the Co-Pol pattern remains centered at broadside (0°) for all frequencies, and the 3 dB beamwidth ranges from approximately 12.8° to 14°, demonstrating good frequency stability across the band which is good for enhancing directionality and angular resolution. Side-lobe levels (SLL) appear around $\theta = \pm 60°$ with amplitudes ranging from –13 to –15 dB relative to the main lobe, which is moderate and acceptable for most practical applications. Some asymmetry and pattern ripple, particularly at 78 GHz, are observed and may result from residual grating lobe effects or slot geometry. Similar co-polarized dominance is observed in the H-plane (Fig. 5 (b)), with cross-polarized levels suppressed by more than $XPD > 24.1$ dB at broadside. The radiation patterns exhibit stable beam direction and minimal side lobes, indicating effective beam shaping and well-controlled polarization behavior across the frequency range. The 3 dB beamwidth is about 109°.

As shown in Fig. 6(a), the antenna achieves a front-to-back ratio of around 30 dB, indicating strong directivity in the broadside direction. The side-lobe level (SLL) also shown in the same figure confirms that grating lobes remain suppressed in the principal E-plane. Slot tapering is employed as an effective technique to reduce side lobes further, especially when increasing the number of slots. Fig. 6(b) illustrates the cross-polarization characteristics, showing minimal cross-polarization levels near the broadside direction. The proposed antenna demonstrates good cross-polarization performance and offers a significantly reduced profile compared to GW antennas reported in [5], [8], and [9].

By adding two additional layers to the conventional three-layer horizontally polarized MLW antenna, the proposed design achieves slant polarization while preserving a compact form factor. With a total height of just 1.6 mm, approximately 3 times thinner than the 4.8 mm GW antenna in [5], this design offers a highly compact and efficient solution for slant-polarized mmWave applications.

The antenna can be fabricated using chemical metal etching, a standard method for MLW antennas. However, using thin metal layers and sub-millimeter slot dimensions introduces unavoidable dimensional tolerances during fabrication. These deviations may result in slight discrepancies between simulated and measured performance. It is essential to incorporate fabrication tolerances into the simulation process to address these effects to ensure robust and reliable design predictions.

A comparison of the proposed antenna with other published designs to evaluate its performance in terms of size, gain, polarization, etc. is shown in Table 2. We provide published work focusing on either MLW, GW technologies, and the realization of either horizontal, circular, or slant polarization. In addition to the antenna's overall strong performance, the use of MLW technology has significantly enhanced its design by minimizing the thickness, contributing to a more compact and efficient structure.

4. Conclusion

A slant-polarized coaxial slot antenna based on gap waveguide (GW) multilayer waveguide (MLW) technology is proposed for automotive radar applications. Simulation results demonstrate its effectiveness for E-band systems, particularly in joint communication and sensing (JCAS), or integrated communications and sensing (ICAS), platforms. A key advantage of the design is its ability to significantly reduce self-interference when paired with an orthogonally polarized counterpart, such as an identical array rotated by 90°. These complementary slant polarizations (±45°) offer electromagnetic and system-level benefits, e.g., enhancing isolation, diversity, and robustness, making them well-suited for advanced mmWave automotive applications. Although this approach introduces some design complexity, the resulting performance improvements often outweigh these challenges.

The antenna exhibits a wide impedance bandwidth of 76 to 81 GHz, ensuring robust and reliable performance across the designated E-band spectrum for automotive radar applications. This wideband operation enables high-data-rate communication and precise sensing, effectively meeting the demanding requirements of modern automotive and industrial environments.

Additionally, the antenna delivers a high-gain, fixed broadside beam, making it well-suited for applications requiring focused and stable signal transmission or reception. This characteristic is particularly beneficial for radar systems and point-to-point communication links, where maintaining high signal integrity, directional accuracy, and spatial isolation is critical to overall system performance.

Overall, the proposed antenna design offers a robust and cost-effective solution by leveraging MLW technology. It provides advantages such as polarization diversity, wide bandwidth, and high gain, while effectively addressing critical challenges including self-interference and signal fidelity. These features make the antenna a compelling candidate for advanced E-band systems in research and real-world deployments.

Acknowledgment

This work has been funded by the H2020-MSCA Project 955629 ITN-5VC. We also appreciate funding from the ELLIIT strategic research environment (https://elliit.se/).

References

[1] C. Waldschmidt, J. Hasch, and W. Menzel, "Automotive radar—from first efforts to future systems," *IEEE Journal of Microw*, vol. 1, no. 1, pp. 135-148, Jan. 2021.

[2] A. Venon, Y. Dupuis, P. Vasseur, and P. Merriaux, "Millimeter wave FMCW radars for perception, recognition, and localization in automotive applications: a survey," *IEEE Transactions on Intelligent Vehicles*, vol. 7, no. 3, pp. 533-555, Sept. 2022.

[3] Q. Ren et al., "An Automotive Polarimetric Radar Sensor With Circular Polarization Based on Gapwaveguide Technology," *IEEE Transactions on Microwave Theory and Techniques*, vol. 72, no. 6, pp. 3759-3771, June 2024.

[4] T. Visentin, "Polarimetric radar for automotive applications," *Ph.D. dissertation, Dept. Elect. Eng., Karlsruhe Institute of Technology*, Karlsruhe, Baden-wuerttemberg, Germany, 2019.

[5] R. G. Zarnagh, A. Haddadi, and A. A. Glazunov, "A Dual Linear-Polarized Gap Waveguide Antenna Element for Radar and Communications at 77 GHz," *2024 18th European Conference on Antennas and Propagation (EuCAP)*, Glasgow, United Kingdom, 2024, pp. 1-5.

[6] P.-S. Kildal, A. U. Zaman, E. Rajo-Iglesias, E. Alfonso, and A. Valero-Nogueira, "Design and experimental verification of ridge gap waveguide in bed of nails for parallel-plate mode suppression," *IET Microwaves, Antennas & Propagation*, vol. 5, no. 3, pp. 262–270, Mar. 2011.

[7] W. Y. Yong, A. Vosoogh, A. Bagheri, C. Van De Ven, A. Hadaddi and A. A. Glazunov, "An Overview of Recent Development of the Gap-Waveguide Technology for mmWave and Sub-THz Applications," *IEEE Access*, vol. 11, pp. 69378-69400, 2023.

[8] R. G. Zarnagh, A. Haddadi and A. A. Glazunov, "A Vertically Polarized Gap Waveguide Array Antenna for Joint Communication and Sensing," *2024 International Symposium on Antennas and Propagation (ISAP)*, Incheon, Korea, Republic of, 2024, pp. 1-2.

[9] Z. Zang, Q. Ren, A. Uz Zaman and J. Yang, "77 GHz Fully Polarimetric Antenna System With Compact Circularly Polarized Slots in Gap Waveguide for Automotive Radar," *IEEE Transactions on Antennas and Propagation*, vol. 72, no. 7, pp. 5578-5588, July 2024.

[10] A. Vosoogh, H. Zirath, and Z. S. He, "Novel air-filled waveguide transmission line based on multilayer thin metal plates," *IEEE Transactions on Terahertz Science and Technology*, vol. 9, no. 3, pp. 282–290, 2019.

[11] A. Vosoogh, A. Haddadi and C. Bencivenni, "Novel Low-loss Coaxial Slot Array Based on Gap Waveguide Technology for E-band Automotive Radar Applications," *2023 17th European Conference on Antennas and Propagation (EuCAP)*, Florence, Italy, 2023, pp. 1-5.

[12] J. -L. A. Lijarcio, A. Vosoogh, C. Bencivenni and A. U. Zaman, "Low-cost Coaxial Slot Array Antenna for E-Band Automotive Corner Radar Applications Based on Gap Waveguide MLW Technology," *2024 18th European Conference on Antennas and Propagation (EuCAP)*, Glasgow, United Kingdom, 2024, pp. 1-5.

[13] M. Sano, J. Hirokawa, and M. Ando, "A hollow rectangular coaxial line for slot array applications fabricated by diffusion bonding of laminated thin metal plates," *IEEE Transactions on Antennas and Propagation*, vol. 61, no. 4, pp. 1810–1815, Apr. 2013.

[14] F. Yang, Y. Rahmat-Samii, "Electromagnetic Band Gap Structures in Antenna Engineering," *Cambridge University Press*, 2009.

[15] C. A. Balanis, "Antenna Theory: Analysis and Design," *Wiley*, 4th ed. Hoboken, 2016.

[16] Z. Zang, A. U. Zaman and J. Yang, "Single-Layer Dual-Circularly Polarized Series-Fed Gap Waveguide-Based Slot Array for a 77 GHz Automotive Radar," *IEEE Transactions on Antennas and Propagation*, vol. 71, no. 5, pp. 3775-3784, May 2023.

[17] R. G. Zarnagh, A. Haddadi, C. Van De Ven and A. A. Glazunov, "A Slant-Polarized Coaxial Slot Array Antenna Based on Gap Waveguide MLW Technology for E-Band Applications," *2025 19th European Conference on Antennas and Propagation (EuCAP)*,Stockholm, Sweden, 2025, pp. 1-5.

[18] J. -L. A. Lijarcio, A. Vosoogh, C. Bencivenni and A. U. Zaman, "Low-Cost Center-Fed Slot Array Based on Gap Waveguide MLW Coaxial Line Technology for E-Band Automotive Radar," *IEEE Transactions on Antennas and Propagation*, vol. 72, no. 7, pp. 5674-5681, July 2024.